Hindawi
Journal of Sensors
Volume 2019, Article ID 8652527, 16 pages
https://doi.org/10.1155/2019/8652527

Research Article

A Sentinel Node for Event-Driven Structural Monitoring of Road Bridges Using Wireless Sensor Networks

Glauco Feltrin[1], **Nemanja Popovic**[1] **and Michał Wojtera**[2]

[1]*Empa-Swiss Federal Laboratories for Materials Science and Technology, Switzerland*
[2]*Department of Microelectronics and Computer Science, Technical University of Lodz, Poland*

Correspondence should be addressed to Glauco Feltrin; glauco.feltrin@empa.ch

Received 7 May 2018; Accepted 19 November 2018; Published 31 January 2019

Academic Editor: Christos Riziotis

Event-driven monitoring policies enable to significantly reduce the power consumption of wireless sensor networks by reducing the recording period to those time intervals that provide valuable data. The resulting longer operation lifetime increase discloses fields of application that require long monitoring periods. This paper presents a structural monitoring system that uses specialized sentinel nodes for detecting possibly heavy road vehicles and for alarming monitoring nodes, which are specialized on strain sensing. Heavy vehicles are identified by estimating nearly in real time height and length of vehicles of a traffic flow by processing data recorded from low-cost ultrasonic and magnetic displacement sensors. Field tests demonstrated that while height detection is very reliable, length detection is too imprecise to discriminate with high success rates between trucks and delivery vans.

1. Introduction

Structural monitoring is increasingly becoming an important tool for assessing existing civil structures since specific information about the state and performance of the structure enables to achieve a more effective and cost-optimized management of civil infrastructure [1]. Inclusion of information obtained from monitoring data has proved to provide more reliable fatigue assessment than purely design model-based methods [2, 3]. Currently, the most significant impediments for a regular application of monitoring in engineering practice are the lack of codified simple procedures for inclusion of monitoring data and the still high costs of monitoring. Cost reduction can be achieved by optimizing the design of monitoring systems in terms of sensor placement, data quality, and minimal monitoring period. Furthermore, monitoring systems that enable a fast mounting contribute to reduction in deployment costs.

Monitoring systems based on wireless sensor networks belong to this category and are expected to have a potential for reducing significantly the deployment costs because the costly and time-consuming cabling is avoided. Since their first appearance in structural monitoring about 15 years ago, wireless sensor networks have shown to be vastly applicable and to provide a high data quality while achieving a sufficiently high operation reliability. Wireless sensor networks are perfectly competitive to tethered monitoring systems for monitoring applications involving low data rates such as monitoring of slowly varying structural processes. This is possible as the hardware has to be operated only periodically and for very short time laps. Monitoring of dynamic processes is much more challenging due to high data rates. Wireless communication of the raw data often exceeds the communication bandwidth and results in a quick depletion of batteries since communication is power-expensive. Furthermore, permanent operation of sensing hardware contributes to power consumption. Frequent maintenance activities such as battery replacements may therefore nullify the cost advantages of WSN over tethered monitoring systems. Both drawbacks could be significantly mitigated by using low-power sensors, signal conditioning circuits, and embedded data processing. Field tests demonstrated

that typical monitoring applications involving dynamic processes can achieve battery replacement periods of several months [4, 5].

An additional interesting concept to extend battery lifetimes is to operate a wireless monitoring system in an event-driven mode. This concept consists in restricting the monitoring period to those time intervals that provide valuable data. Since outside these time intervals there is nothing interesting to monitor, the sensing hardware can be switched off and the sensor node can be set in a low-power sleep state. A typical example of an event-driven operation mode is strain cycle monitoring on a railway bridge. Strain cycles being relevant for fatigue life assessment are only expected to occur when a train is crossing the bridge.

An event-driven recording policy is a standard feature on tethered commercial monitoring systems. On these systems, since power consumption is uncritical, sensing, analog-to-digital conversion, and data recording on a volatile memory are performed permanently with all sensors. Permanent data recording is induced by a triggering mechanism that often relies on exceeding a given signal threshold of one specific sensor. A similar approach is also feasible with wireless sensor networks and can be a simple and effective method if the operation period is short [6].

A better performance in terms of energy efficiency can be achieved, if the often power-intensive sensing hardware can be switched off most of the time. Such a concept requires an auxiliary event sensing mechanism that switches on the primary sensing hardware if an event is detected. Energy efficiency can be achieved if the event sensing hardware, which has to operate permanently, consumes significantly less power than the primary sensing hardware does. Sensor nodes equipped with such an auxiliary event sensing feature have been investigated for different monitoring applications [7–10]. Such a mechanism was investigated for strain sensing on railway bridges [11]. Vibrations induced by approaching trains were sensed by an ultra-low-power acceleration sensor and used for event detection. The energy-expensive strain sensing hardware was switched on when the vibration amplitude exceeded a threshold. This approach was simple and effective for saving power but had three important drawbacks. First, the acceleration sensor and the associated signal conditioning hardware increased the costs of a sensor node. Second, since the sensor nodes had to be placed on the bridge, data recording was started relatively late with respect to the arrival time of the train. The initial part of the records was therefore biased by transient signals that were induced by switching on the strain sensing hardware such as heating of the strain gauge and charging of capacitors in the electronic circuits of the strain sensing hardware. Third, since the auxiliary event sensing hardware was integrated in the sensor node and each node was placed in a different position of the bridge, each node had to be set up with a specific threshold. Such a configuration is quite time-consuming.

Recently, Popovic et al. [12] proposed an auxiliary triggering mechanism that does not have these drawbacks. They separated physically the two functionalities, event detection and monitoring, which Bischoff et al. [11] implemented within a sensor node, by introducing sentinel nodes, which are specialized on train detection, and monitoring nodes, which are specialized on sensing and recording the physical quantities. Once a sentinel node detected an imminent event, it notifies the monitoring nodes by broadcasting alarm messages throughout the network. The monitoring nodes were operated in a low-power sleep mode and woken up periodically to listen for alarm messages. Only upon receiving such an alarm message did the monitoring nodes turn on their sensing hardware and start recording the event. After completion of recording, the monitoring node switched off the sensing hardware and went back to sleep mode. A field test on a railway bridge demonstrated that event detection and event notification were reliable and fast and provided a significant extension of battery lifetime [12].

The key aspect for successful application event detection with sentinel nodes is the reliability of event detection. Failures in detecting an event lead to data loss that may bias the assessment of the structure. False alarms waste power for sensing, recording, and processing data that is valueless. Detecting an event is sometimes rather straightforward. Popovic et al. [12] sensed rail vibrations for detecting trains. Each time the vibration amplitudes exceeded a given magnitude, the monitoring nodes were notified. Only trains can produce such high vibration amplitudes of the rail, and only trains were inducing strain amplitudes that are significant for monitoring. The likelihood of missing a train or incurring into false alarms was therefore very small.

The event detection is much more complex on road bridges. On these bridges, only trucks or buses are causing effects that are worth to be recorded. Cars and delivery vans are very often too light to produce effects that are of any interest. Therefore, sentinel nodes must have the ability to discriminate trucks and buses from all other vehicles. This discrimination has to be performed nearly in real time and with sensing devices that are sufficiently low-cost, low-power, and quickly deployable. Modern automatic traffic counting or toll collection stations as well as weight-in-motion sensors that are regularly used along roads are very effective in categorizing vehicles. However, their high costs and long installation times would frustrate all cost advantages provided by using wireless sensor networks.

In this paper, a low-cost and low-power sentinel node is proposed that is able to identify in real time and with a good hit rate trucks and buses within a vehicle flow. Section 2 addresses the sensors and algorithms for detection of vehicle height and the estimation of vehicle length. Section 3 analyzes the algorithms and provides suitable value ranges for the parameters. The field test is described in Section 4 and its results in Section 5. Finally, Section 6 draws the conclusions.

2. Event Detection

2.1. Concept. What makes the identification of heavy vehicles within a traffic flow challenging is the discrimination between heavy and light vehicles. Since recording vehicle weight is excluded because of high hardware and deployment costs, the discrimination has to be performed by measuring other physical quantities of a vehicle which are correlated with the weight. Furthermore, to be compatible with the

major paradigms of monitoring with wireless sensor networks, a solution has to satisfy three requirements:

(i) Sensing should be performed with low-cost and low-power sensors

(ii) Truck recognition by embedded data processing should be simple and fast

(iii) Sentinel node deployment should be flexible, fast, and low-cost

The train detection method used by Popovic et al. [12] stands for an event detection system that meets these requirements. It is based on vibration sensing, which was implemented with a low-power MEMS accelerometer, and the identification, which is based on the exceedance of an amplitude threshold in two consecutive records, is achieved with a very simple and fast data processing algorithm.

Unfortunately, extending this simple approach to discriminate heavy road vehicles was not successful. Heavier vehicles generally generate greater soil vibrations than light vehicles do, but defining a reliable threshold turned out to be difficult. A too low threshold generates many false-positive identifications, and a too high threshold misses too many heavy vehicles. Similarly, the same drawbacks suffer the identification of heavy vehicles based on noise induced by vehicles.

In this paper, truck recognition is performed by estimating the size of a vehicle. Trucks and buses differ in height and length substantially from passenger cars and delivery vans. While trucks' height exceeds 3 m, the height of cars and delivery vans is often smaller than 3 m. The length of heavy trucks is seldom smaller than 7 m while cars and delivery vans do usually not exceed 6 m in length. These gaps within vehicle categories can be exploited to discriminate heavy from light vehicles.

Clearly, detecting a large vehicle does not assure to have detected also a heavy vehicle since it may travel without freight. Figure 1 displays measurements of vehicle length and weight recorded in a weight on motion station in Switzerland over one year. Each vehicle heavier than 3.5 tons was recorded. Despite the significant scattering, the data shows that the weight of a vehicle increases with increasing length. According to Figure 1, vehicles shorter than 5 m only very rarely (0.2% of vehicles) exceed a weight of 10 tons. For vehicles with a length smaller than 7 m, the likelihood to exceed 10 tons is 10 times greater, namely, 3.3%. The likelihood increases with increasing vehicle length (25% for 10 m and 43% for 15 m).

In Western countries, the maximum weight of cars and delivery vans, which represent the majority of vehicles travelling on roads, is regulated and usually does not exceed 3.5 tons. Delivery vans belonging to this vehicle category may exceed a height of 2.5 m. Small trucks whose admissible weight exceed by far 3.5 tons exhibit a height which is in the same range.

2.2. Height Detection. The main goal of height detection is to discard cars and delivery vans. It should operate like a filter and report only vehicles that exceed a given height threshold. In this context, knowing the exact vehicle height is not important. On the other hand, height detection should be able to distinguish on which lane the detected vehicle is driving since on roads with two lanes with opposite driving directions, only vehicles travelling on one lane will eventually cross the bridge. These requirements suggest using a sensor that enables to detect a travelling object of a given height situated within a defined distance range.

In this work, height detection was implemented with the ultrasonic noncontact object detection and ranging sensor HRXL-MaxSonar MB7360 [13]. By mounting the sensor at a height of, e.g., 2.5 m, above the road pavement, it detects obstacles exceeding ca. 2.20 m in height since with a full horn the diameter of the beam shape is about 60 cm. This sensor enables to detect objects up to a distance of 5 m with a resolution of 5 mm. Distance is estimated by measuring the travelling time of a short ultrasonic pulse, which was emitted by the sensor, reflected back by the obstacle and sensed by the sensor. An internal temperature compensation accounts for the influence of air temperature on wave speed in air. Since distance measurement is used for identifying only on which lane the vehicle is moving, distance accuracy is of minor importance. An important criterion for choosing the sonar was low-voltage operability and power consumption. With an input voltage of 2.7 V to 5.5 V, its average power consumption is about 7 mW at 3 V. These figures are suitable for operating the sonar with a battery-powered sensor node.

The procedure for height detection is very simple. An internal timer of the sensor node, which is set to fire with constant pulse rate (e.g., 7.5 Hz), triggers the measurements. Upon the return of the emitted wave, the sensor internally calculates the time of flight and the distance to the reflecting object and sets the analogue output to a value that is proportional to this distance. This value is kept constant until the next measurement is triggered. In case the emitting pulse does not bounce back from an object, the analogue value will be set out of range of the A/D converter (e.g., 4095 on a 12-bit converter).

To be sure that the signal did not bounce back from the vehicle passing in the other direction, each calculated distance is compared with a distance threshold. A lower distance means there is a high vehicle passing in the direction of interest. When the vehicle has been detected, the algorithm checks a flag which indicates whether the notification has already been issued. If this flag is not set, the algorithm sets the flag and notifies the detection by setting the general I/O interrupt line to 0 for the duration of 100 ms. Each of the following detections will be ignored as long as the flag is set. The flag will be cleared upon appearance of the first nondetection event.

2.3. Length Estimation. Length estimation of a travelling vehicle is significantly more complex than height detection. Since the vehicle is moving, length estimation can only be achieved by estimating simultaneously also its speed. In fact, the signal of a short vehicle travelling at low speed may otherwise be confused with a long vehicle travelling at high speed. Today, inductive loop detectors (ILDs) are the most

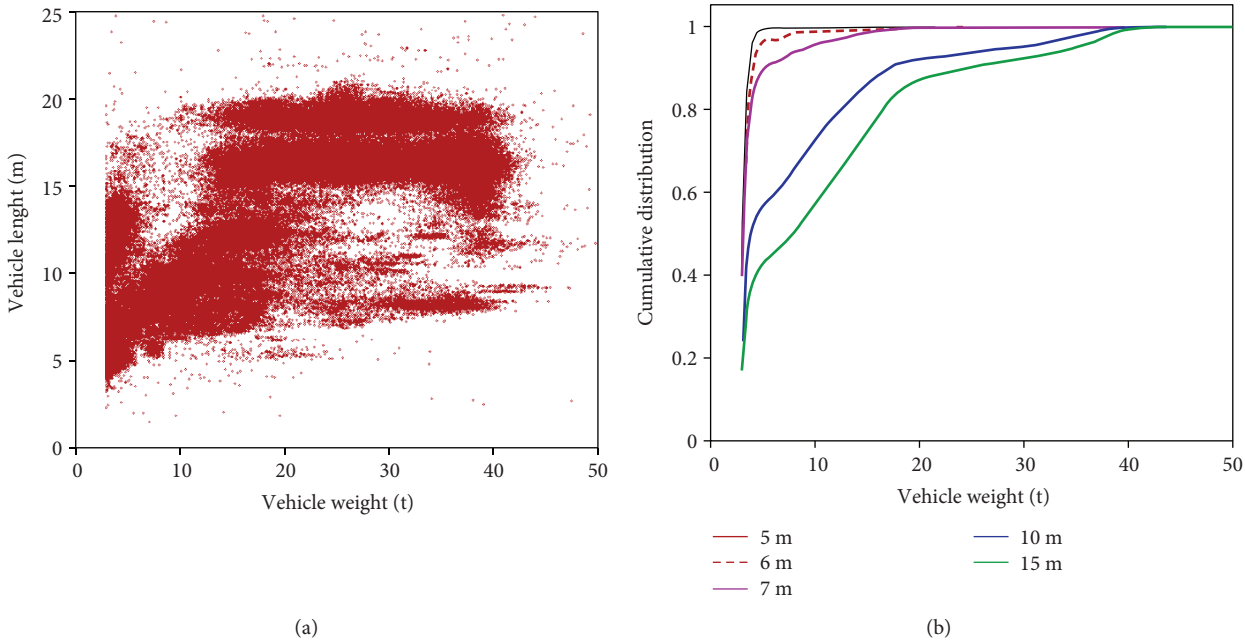

Figure 1: Correlation between vehicle weight and length and cumulative distribution of vehicle weight for vehicles with different lengths.

commonly used sensors for traffic classification in permanent automatic traffic count stations [14]. Vehicles passing over a loop or stopped within the loop induces eddy currents in the wire loop which can be measured with a suitable signal conditioning circuit. Typically, these systems operate with two loops (dual-loop detectors) and the speed of a vehicle is estimated by computing the ratio of the distance between the loops to the time delay of the signals generated by the loops [14]. The vehicle length is finally estimated by multiplying the signal duration with the speed. Such ILDs operate very reliably but, unfortunately, do not fit into the low-power, low-cost, and rapid deployment paradigm of monitoring with wireless sensors networks.

Magnetic sensors have been used with some success for traffic counting, vehicle classification, and speed estimation. In analogy to IDLs, the mass of ferromagnetic material of passing vehicles induces a detectable disturbance of the magnetic field. While speed estimation was quite reliable with an error of a few percent, the success rate for vehicle classification for adjacent vehicle classes ranged between 65 and 88% [15–17]. A classification accuracy of more than 97% could be achieved for low-speed congested traffic by using a single magnetoresistive sensor [18].

In this work, vehicle length is estimated using low-power and low-cost magnetic displacement Honeywell HMC1501 sensors. The Honeywell HMC1501 magnetic displacement sensor [19] is a low-voltage sensor which can be operated with an input voltage ranging from 1 to 25 V. Its power consumption at 3 V is about 4 mW. The sensor is used in industry for detecting ferromagnetic objects.

Typical signals produced by car and trucks are displayed in Figure 2. The signal pattern depends on the vehicle's characteristics but also on the distance between the vehicle and the sensor, which varies from vehicle to vehicle. Since these sensors are typically used as near range proximity sensors (up to 20 mm), the much more articulated signal of the truck may depend on the distance of the vehicle from the sensor rather than on the characteristics of the vehicle. In fact, the signals displayed in Figure 2 differ substantially from typical signals obtained with ILDs, whose amplitudes usually do not change sign [14]. Since for length estimation only the duration of signal disturbance matters, signals of magnetic displacement sensors can still be suitable for our goal.

The characteristics of these sensors to detect objects within an angular range of 45° tend to overestimate the length of a vehicle. A vehicle appears longer the greater the distance is between the vehicle and the sensor. Theoretically, the length increases by twice this distance. With increasing distance, however, the signal amplitude decreases and mitigates the length overestimation.

Vehicle speed and length estimation is performed using three HMC 1501 magnetic displacement sensors that are placed along a straight line. A sensing sector (the distance between the first and third sensor) of 8 meters has proven to be precise enough even for high speeds. At lower speeds, however, the distance between vehicles can be rather small thus increasing the likelihood of having two vehicles within the sensing sector. A third sensor in the middle of the sensing sector improves the ability to distinguish between different vehicles and contributes also to the improvement of the precision of length estimates.

The most straightforward approach for recognizing a passing vehicle is to use directly the signal amplitude and determining how long a threshold was exceeded. This threshold should be just greater than the noise level of the sensing unit in order to achieve a high resolution. Because of the noise, the threshold cannot be checked with just the most recent signal value in order to avoid false detections. Averaging several values provides a better estimate of the signal amplitude, but its number should be small since they

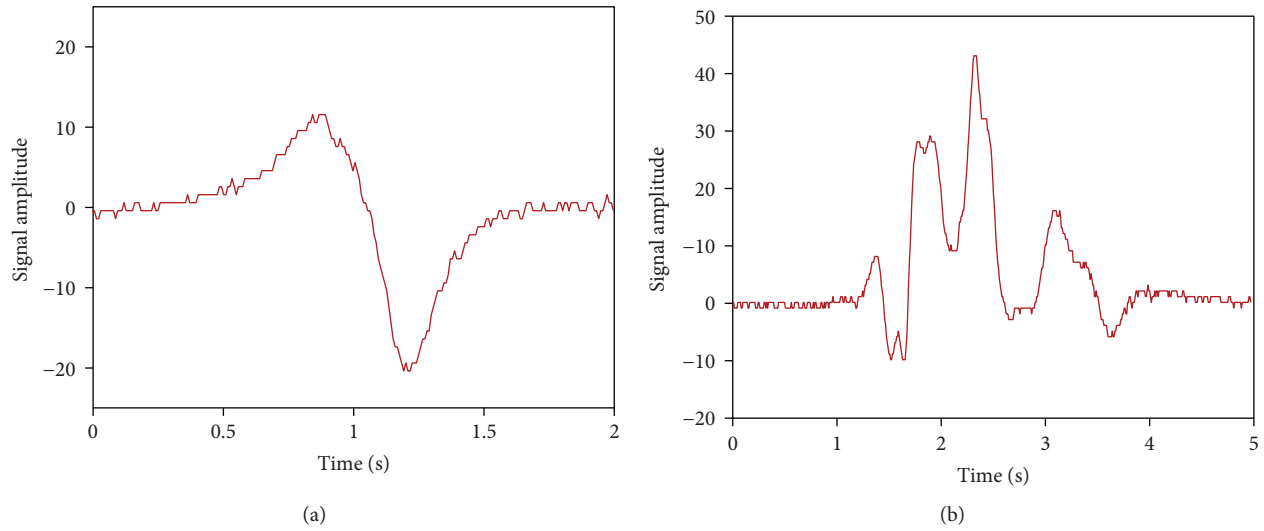

Figure 2: Signal induced by a car (a) and by a truck (b).

determine the time granularity. Using signal amplitude implicitly assumes that it is always possible to define a reference value (e.g., zero) and that this reference value is constant with time or can be redefined at any time. The sensing unit showed small short-time trends in its signal that required redefining autonomously the reference value with a high frequency. Because of the unpredictability of traffic flow, reference value resetting is nontrivial and requires a permanent switching between length detection and reference value resetting algorithm.

Reference value resetting can be avoided by using the signal gradient. In order to cope with the noise, the gradient has to be estimated with a time interval. Similarly to signal value estimation, the interval should be short in order to obtain a good time resolution. The drawback with the signal gradient is that it may depend on vehicle speed. If the signal strength does not depend significantly on signal speed, the slower the vehicle the smaller the signal gradient is. In this study, the signal gradient was used for vehicle length estimation.

The length estimation algorithm is organized in two layers. The first layer addresses the sensor-wise processing and data collection while the second layer combines the information of the three sensors and finally estimates the vehicle speed and length.

2.3.1. First Algorithm Layer. The first layer which deals with the data of a single sensor is summarized in Figure 3. The signal of each magnetic displacement sensor is sampled with a constant frequency (e.g., 123 Hz). This continuous data stream is organized in data blocks containing a predefined number of samples (e.g., 4 samples). Each sensor features a state variable, a wait counter, and a start and end time. The state variable takes the values detecting (threshold exceeded) and nondetecting (threshold not exceeded) while the wait counter takes values between 0 and a user-defined upper limit.

The processing of the data blocks is simple and consists of finding its maximum and minimum and checks whether their difference (gradient) is greater than a user-defined threshold. The algorithm starts a processing loop by reading the front data block and checking for the threshold. If the threshold is exceeded, the algorithm first checks if the sensor is in detection state. If not, the algorithm assumes that the threshold exceedance corresponds to the beginning of the passage of a new vehicle and switches the state variable to detection state. Afterwards, the current time, in terms of the local timer value, is saved as start time and as end time. Finally, after the waiting counter is initialized to 0, the algorithm starts a new processing loop.

If at threshold exceedance the sensor is in the detection state, the end time from a previous loop will be overwritten with the current local time and the waiting counter will be reset to 0.

On the other hand, if the threshold is not exceeded, the algorithm performs an operation only if the sensor is in detecting state. In that case, the waiting counter will be increased by one. This corresponds to a situation where the signal changes are small, but the vehicle has still not completely passed the sensing range of the sensor. Afterwards, the waiting counter is checked against the limit value, which represents a timeout condition (e.g., 0.5 s) separating two distinct vehicles. When the limit value is matched, the sensor reports the initial and end time values to the second algorithm layer, switches the state to nondetecting, and restarts the processing loop.

2.3.2. Second Algorithm Layer. While the first algorithm layer handles the data recorded by one sensor, the second algorithm layer is designed to combine the three outputs generated by the first algorithm with the goal of finally estimating the vehicle speed and length. The basic structure of the algorithm is straightforward since it has to combine the three pairs of start and end times generated by the first algorithm layer (Figure 4). The speed is finally estimated by

$$v = \frac{D_{jk}}{\Delta t_{jk}} = \frac{D_{jk}}{t_j - t_k}, \quad (1)$$

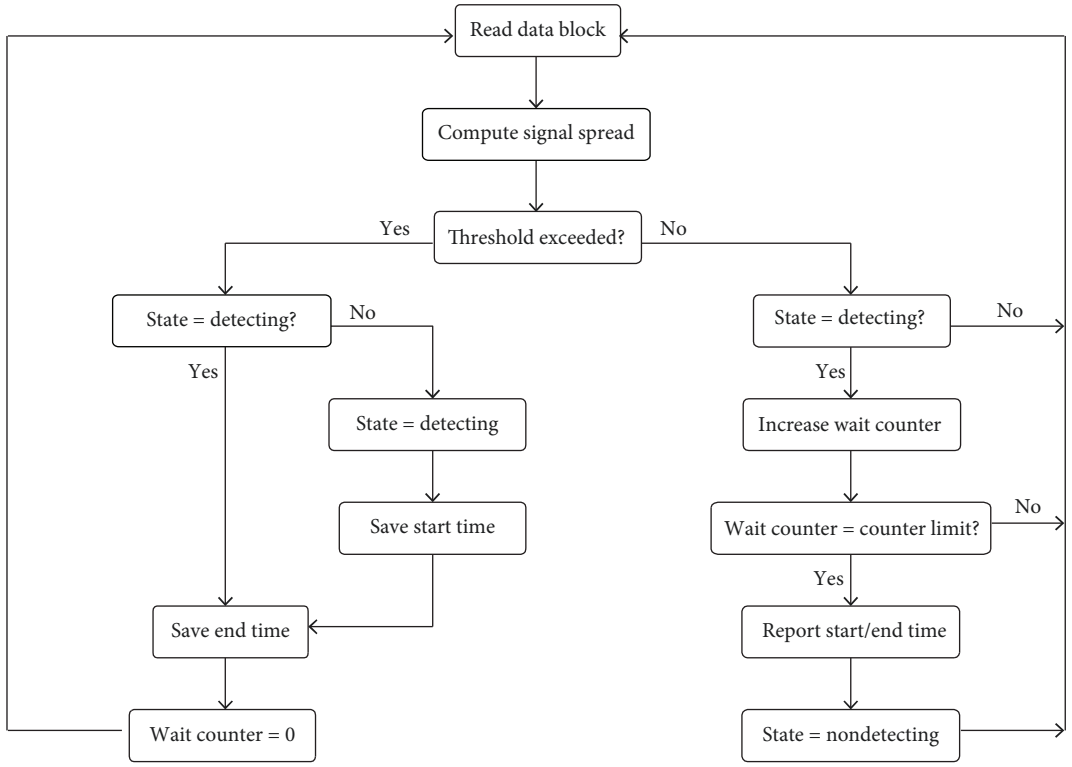

Figure 3: First algorithm layer.

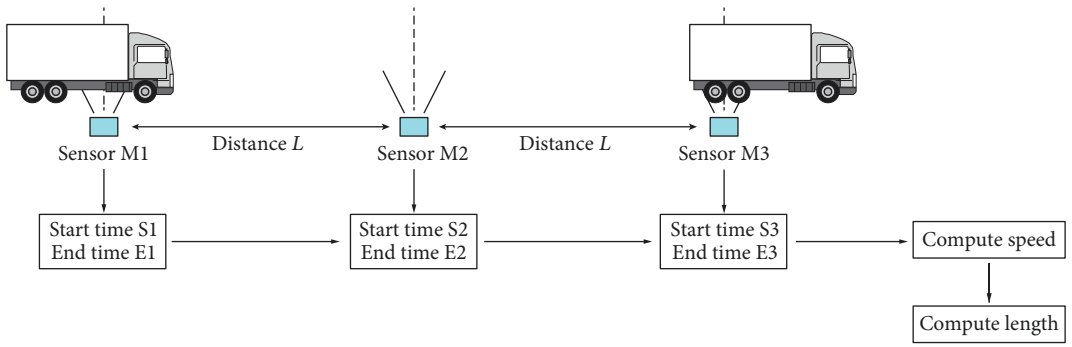

Figure 4: Second algorithm layer.

where D_{jk} is the distance between two magnetic displacement sensors and Δt_{jk} is the time interval between the respective start or end time. The indices j and k refer to the sensors and can take the value 1, 2, or 3 (clearly, $j \neq k$). Once the vehicle speed is estimated, the vehicle length L_v is computed by

$$L_v = \frac{1}{3} v \sum_{j=1}^{3} \tau_j = \frac{1}{3} v \sum_{j=1}^{3} \left(t_{e,j} - t_{s,j}\right), \tag{2}$$

where τ_j is the signal duration that results from the end and start times ($t_{e,j}$ and $t_{s,j}$), respectively.

If each sensor would operate reliably, there would be little to add. Testing experience, however, showed that sometimes a sensor missed a vehicle. The algorithm has to cope with such situations in order to avoid wrong length estimations.

First, we consider the case that the first sensor has detected a vehicle. Whenever it has finished the detection process, a data object is created which contains the start and end times. Subsequently, the registers associated to this sensor are initialized for detection of the following vehicle and a first detection timer is created and initiated. The detection timer has an expiration time as threshold parameter. Its purpose is to give to sensor 2 an upper time limit for detecting the same vehicle. If the time limit is exceeded, the algorithm assumes that sensor 2 was unable to capture the vehicle.

If the second sensor detects a vehicle before the detection timer of the first sensor expires, the start and end times of the second sensor are copied into the data object.

If the second data object was created because the first detection timer had expired, the data associated to the second sensor will contain zeros, so that the final estimation will be made without this information. In both cases, the registers associated to the second sensor, the first data object and the first detection timer are released for enabling the detection of a following vehicle, and a second detection timer will be created and initialized. The same procedure is finally applied with sensor 3.

If sensor 1 has not detected a vehicle when sensor 2 has completed detection and misses the data object for creating the second data, the algorithm assumes that sensor 1 has failed to detect the vehicle, creates a data object, sets the start and end times of the first sensor to 0, and copies its start and end times into the data object. A detection timer is then created and initiated, and the process continues as described in the previous paragraph. If neither sensor 1 nor sensor 2 detects a vehicle, the algorithm creates a data object containing only the start and end times of sensor 3.

After the third sensor reports its data or when the second detection timer expires, the data of the data object is used for estimating the speed and length of a vehicle. If at least two sensors have nonzero data, it is possible to estimate the speed according to Equation (1). In case that sensors 1 and 3 have captured the event, the speed is calculated using their data since the longer distance provides a better estimation. If the first or third sensor does not detect a vehicle, the speed is estimated with the data of the second sensor and either the data of the first or third sensor. If two sensors miss a vehicle, the speed cannot be estimated and an error message is reported.

Once the speed is estimated, the length of the vehicle is computed using Equation (2) for each magnetic sensor that detected a vehicle and the resulting vehicle lengths are averaged.

2.4. Truck Detection. The truck detection algorithm links the data of the height and length estimation for deciding if the detected vehicle is a truck or not. Decision-making is fairly simple: if within the same time frame a high and long vehicle is detected, the vehicle is assumed to be a truck (Figure 5). Both actions, detecting a long vehicle or detecting a high vehicle, set detection flags, and the associated timers are restarted. Since height and length detection occurs independently at different times, they are not synchronized. Whenever a flag is set and a timer is restarted, the algorithm checks if the complementary flag is also set. If this flag is set and the time difference between the two timers is smaller than a user-defined threshold, an alarm is triggered and the detection flags are cleared.

3. Analysis of the Truck Detection Algorithm

The truck detection algorithm contains several parameters whose values need to be defined according to the site-specific conditions. Since these parameters affect the performance of the algorithm, a brief analysis is performed to study their effect. The pulse frequency of the sonar is the only parameter of relevance in height detection since the high accuracy of position measurement enables a safe identification of the lane. In the length estimation algorithm performance, relevant parameters are the sample size, the threshold and the counter limit of the first algorithm layer, and the detection timer of the second algorithm layer.

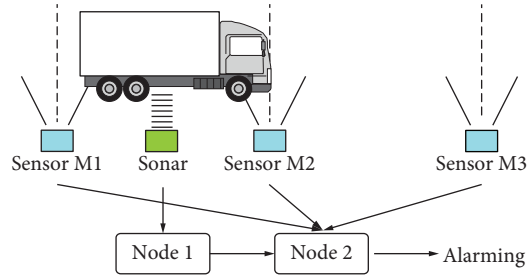

Figure 5: Truck detection.

3.1. Pulse Frequency. The sonar can be operated with a variable pulse rate up to maximum 7.5 Hz. Depending on the vehicle's length and speed, a vehicle is usually hit by several pulses. The resolution of the distance Δl between pulse hits depends on the speed of the vehicle and is given by

$$\Delta l = \frac{v}{f}, \tag{3}$$

where v is the speed and f is the pulse frequency. The hit distance at a speed of 80 km/h with a pulse frequency of 7.5 Hz is 3 m. Equation (3) provides a criterion for choosing a minimum pulse rate for making sure that high vehicles greater than a given length L_v and travelling with a specific maximum speed v_{max} are safely detected (at least one pulse is reflected by the vehicle):

$$f > \frac{v_{max}}{L_v}. \tag{4}$$

Shorter vehicles may also be detected, but the probability is smaller than one:

$$p = \frac{f}{v_{max}} L_v \leq 1. \tag{5}$$

Since the minimum vehicle length L_v is in practice a constant, Eq. (4) states that the pulse frequency should increase with increasing vehicle speed. To detect a vehicle with a length of 8 m on a road with a speed of 80 km/h, the pulse frequency should be greater than 2.8 Hz. This figure is well within the maximum pulse frequency range of the sonar sensor (7.5 Hz). Clearly, battery lifetime would also benefit from using a low sampling frequency.

3.2. Sample Size. The sample size affects primarily the time resolution, since the start and end time markers are set after processing the data blocks (Figure 3). Therefore, for a given sampling rate, the greater the sample size the coarser the time resolution is. The uncertainty induced by the time resolution

can be estimated by applying error analysis. The vehicle speed v is given by

$$v = \frac{L}{T}, \tag{6}$$

where L is the distance between two magnetic displacement sensors and T is the time interval a vehicle needs to cover the distance L. Since the focus is to estimate the uncertainty that is induced by the sample size, L is assumed to be a constant parameter. This assumption is reasonable since L can be measured with much higher precision than T. The error of speed estimation Δv induced by a variation ΔT is

$$\Delta v = \frac{L}{T^2}\Delta T = \frac{v^2}{L}\Delta T. \tag{7}$$

The speed uncertainty is therefore proportional to the time resolution ΔT. The uncertainty increases with the square of the speed and diminishes with the distance L.

The vehicle's length estimation l is given by

$$l = v \cdot \tau, \tag{8}$$

where τ is the time period determined by $\tau = t_{\text{end}} - t_{\text{start}}$. In this case, v as well as τ are subjected to uncertainties so that

$$\Delta l = \sqrt{\tau^2(\Delta v)^2 + v^2(\Delta \tau)^2}. \tag{9}$$

Replacing Δv with Eq. (7) and $\Delta \tau$ with ΔT and after several manipulations yields

$$\Delta l = v\,\Delta T\sqrt{1 + \frac{l}{L}}. \tag{10}$$

Equation (10) shows that the coarser the time resolution is, the more imprecise the length estimation is. Since the uncertainty is proportional to the speed, the block size should decrease on roads with high speeds in order to keep the uncertainty within an acceptable range. The uncertainty can also be reduced by increasing the distance L between the sensors. Its effect is however attenuated by the square root.

3.3. Detection Threshold. For a given sample size, the detection threshold regulates the start and end times (Figure 3) and therefore the period τ. Ideally, the data blocks with exceeded threshold should cover the full length of the magnetic sensor signal induced by a vehicle. Because of the counter limit, which allows for a certain number of gaps between data blocks exceeding the threshold, this is not strictly necessary. In fact, magnetic sensor signals may have periods with small signal changes. Nevertheless, the requirement to reduce the sample size potentially implicitly reduces also the spread between the greatest and smallest values within a data block. Choosing a small sample size increases the likelihood to not exceed the threshold with the effect to completely miss vehicles or to split one long vehicle into shorter ones. The shorter the sample size, the smaller the threshold should be. The noise of the signal, however, sets a lower limit to the threshold and implicitly also a lower limit of the sample size.

Figure 6 shows the signal induced by a vehicle and the average signal spread that result from block sizes 3 and 8, respectively. The average signal spread considers that the initial point of a data block varies and therefore induces different signal gaps. It was computed by averaging the spreads that result by considering each data point within a data block as an initial point. Figure 6 shows that a block size of 3 produces significantly smaller signal spreads than a block size of 8. The signal spreads due to signal noise are, as expected, generally smaller with a block size of 3. The signal spreads associated to a block size of 3 are often smaller than the threshold. With a block size of 8, signal spreads smaller than the threshold occur only at about 1 s. The detection gap is about 0.3 s for a block size of 3 and 0.25 s for a block size of 8. Figure 6 depicts also the signal widths and shows that with a block size of 3 the signal width is shorter, since the first time a threshold is exceeded occurs later as with a block size of 8. By reducing the threshold from 3 to 2, the signal width can be extended. This would work for a block size of 3 since the gap to signal spread due to noise is large enough. For a block size of 8, reducing the threshold to 2 would generate spurious detections which depending on the counter limit could generate virtual vehicles.

At higher speed, the signal spread is generally greater compared to smaller speeds since the signal gradients are greater (Figure 7). In fact, the signal spread with data block 3 is smaller than the threshold on a smaller number of data blocks and the signal spread with data block 8 never goes below the threshold. The occurrence of detection gaps is therefore less critical. The detection width with a block size of 3 is still shorter than with a block size of 8, which in this case agrees very well with the complete relevant signal period. This outcome suggests that length estimation tends to be more reliable with increasing vehicle speeds.

The signals displayed in Figures 6 and 7 demonstrate that, especially at low speeds, significant detection gaps may occur. The goal of the counter limit is to assemble the several separated parts made of contiguous detections in order to cover the full signal width induced by a vehicle. An additional goal of the counter limit is to identify vehicles. The counter limit should therefore be large enough to promote the assembling process but without confusing several consecutive short vehicles into one long vehicle. Clearly, a too small counter limit tends to confuse a long vehicle with two consecutive short vehicles.

3.4. Counter Limit. A sensible selection of a counter limit should base on driver habits. Figure 8 displays recorded time gaps up to 5 s between two vehicles on the slow lane of a Swiss highway. Time gaps seem not to markedly depend on vehicle speed. This result is confirmed by Figure 8, which shows the cumulative distribution of time gap for vehicles driving up to a given speed. For time gaps up to 1 s, the different distributions do not show significantly different patterns. About 1% of vehicles have a time gap smaller than 0.5 s. Such a time gap would probably be a good candidate for defining the

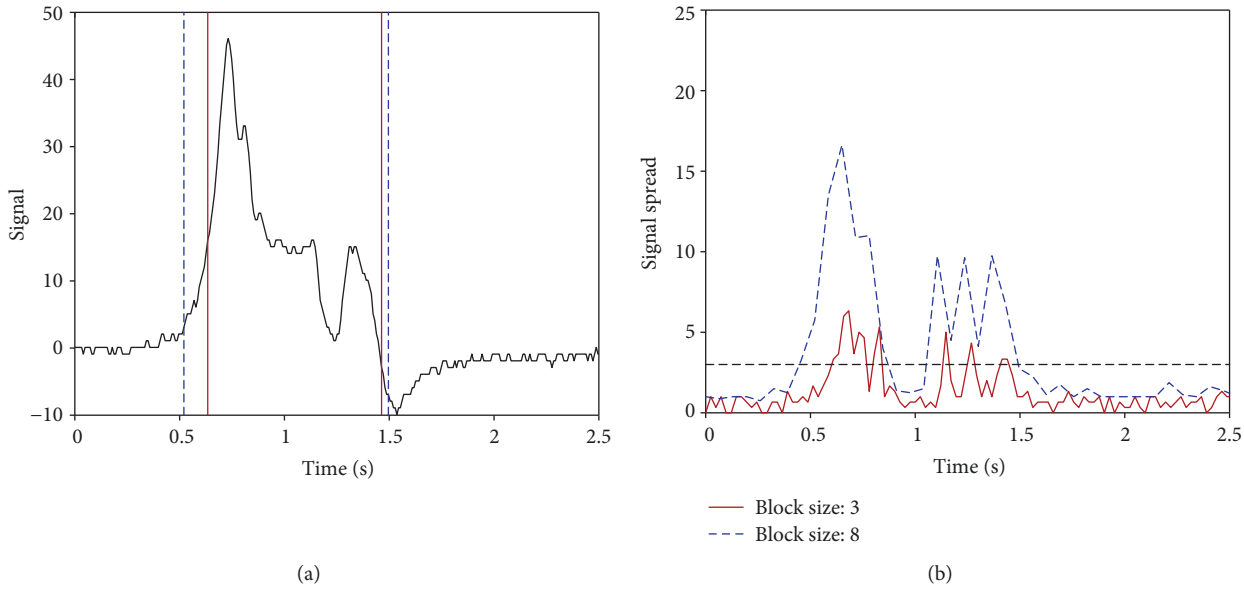

Figure 6: Signal and signal spread of a vehicle with low speed.

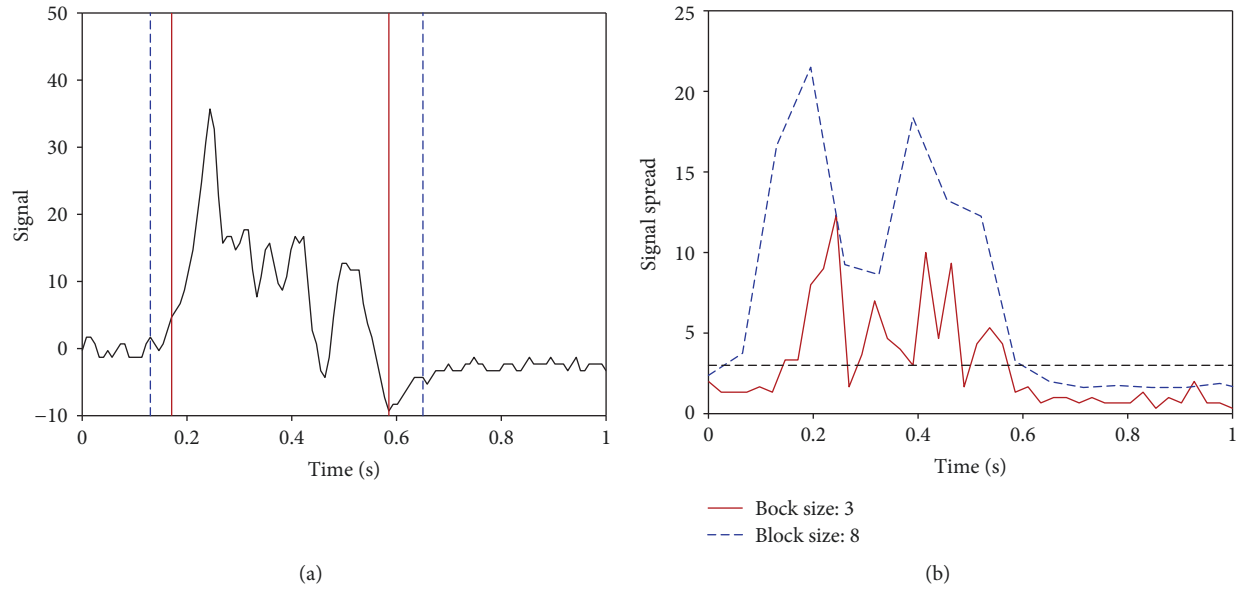

Figure 7: Signal and signal spread of a vehicle with high speed.

counter limit in town roads since Figure 6 demonstrates that time gaps of 0.3 s may occur.

A failure rate of 1% is still acceptable when considering that an error generates a virtually long vehicle. In case of two cars, no alarming will be performed since the height threshold is not exceeded. In case the height threshold is exceeded, if one of the vehicles is a heavy truck there is no error from a strain recording perspective since a heavy vehicle is involved. A false alarm would only occur if two delivery vans or small trucks would be involved. Traffic data reveals that within the population of high vehicles only 3.5% of delivery vans or small trucks are followed by another delivery van or small truck. This small percentage further reduces the likelihood of false alarms to about 0.04%. On the other side, drivers of delivery vans or small trucks tend to keep a significantly smaller distance to the front vehicle than the average since about 4% show up with a time gap smaller than 0.4 s. This percentage increases to more than 5% if the front vehicle is a delivery van or small truck. Even with such figures, the failure rate is very small, namely, about 0.2%.

This analysis suggests that a time gap of 0.5 s for setting the counter limit is a reasonable choice. On roads with speed limits of 80 km/h and more, the time gap could be reduced to 0.4 s or even 0.3 s without incurring into a significant failure rate since at higher vehicle speeds signal time gaps are generally smaller. Nevertheless, the analysis reveals that large time

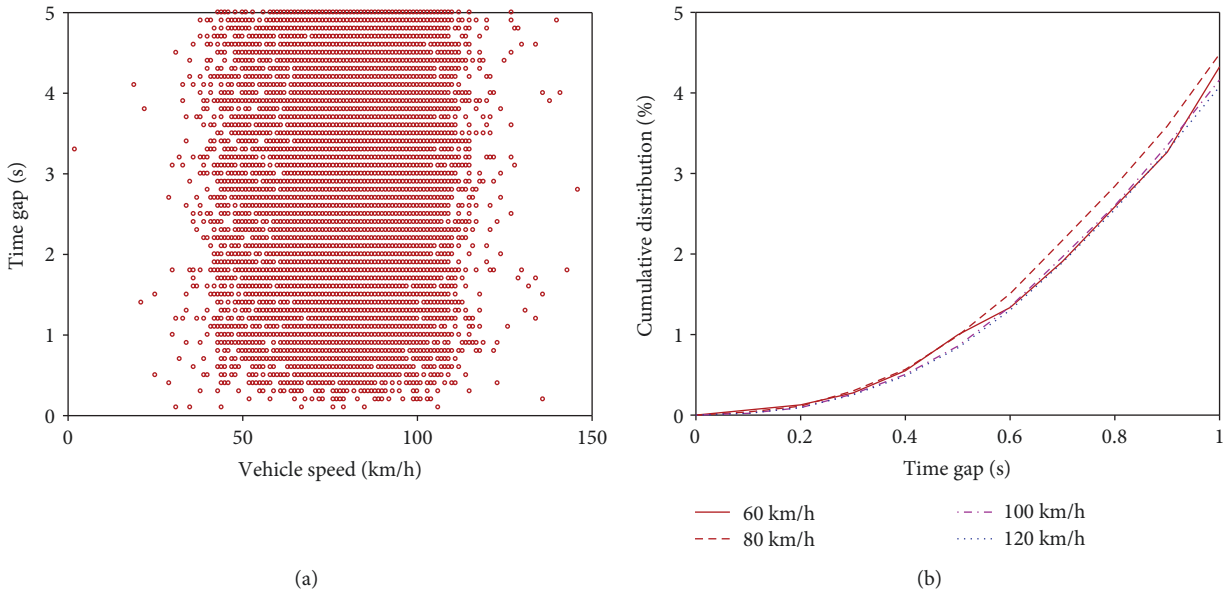

Figure 8: Intervehicle time gap versus vehicle speed and cumulative distribution of intervehicle time gaps.

gaps have a better error redundancy than small time gaps which increase the risk of splitting a long vehicle into two virtual small vehicles and thus suppressing the alarm.

3.5. Detection Timer. The goal of the detection timer is to consider that the vehicles cross the sensing area of the magnetic sensors not simultaneously but time-delayed. This time delay is given by the distance L between two magnetic sensors and the vehicle speed v:

$$\Delta\theta = \frac{L}{v}. \tag{11}$$

The threshold of the detection timer should therefore be greater than $\Delta\theta$; otherwise, the timer would prevent a regular detection of a vehicle by the subsequent sensor. The threshold should be smaller than twice $\Delta\theta$ in order to make sure that the timer expires before the third sensor reports the detection. A reasonable choice of the detection timer threshold is a value in the range (1.25–1.75) $\cdot \Delta\theta$. The gap of the lower bound to $\Delta\theta$ and $2 \cdot \Delta\theta$ considers that the signal length may be different between the sensors. In general, it is better to choose a value close to the upper bound in order to accommodate for smaller vehicle speeds than the speed limit.

For a road with distance of 4 m between two magnetic sensors, a detection timer threshold of 0.3 s covers the speed range of 60 to 80 km/h.

4. Field Test

The goal of the field test was to perform a proof of concept of the sentinel node and monitoring system under real-world operating conditions. The main focus was on the performance of the sentinel node to identify heavy vehicles within a traffic flow. Aspects concerning the performance of the network (event hit rate, data loss, and power consumption) were not studied, since a reliable investigation would have required a much longer testing period.

The test was performed on a small bridge that crosses the river Reppisch and is situated in the industrial area of Dietikon, Switzerland (Figure 9). The post-tensioned concrete bridge has a span width of 19.0 m and a width of 10.5 m. The selection of this bridge was motivated by the relative high truck density (50 trucks per hour in average during working hours), and the small height over the river ground together with low water level provides a very good accessibility for mounting sensors on the bridge. The bridge, which was erected in 1957, is still in a very good condition.

4.1. Monitoring Set-Up. An overview of the test deployment is displayed in Figure 10. The deployment consisted of 1 sentinel node, 2 relay nodes, and 3 monitoring nodes. The sentinel node was placed 144 m in front of the bridge with the three monitoring nodes. The speed limit of the road was 50 km/h. At that speed, a vehicle needs 10 seconds to cover the distance between the sentinel node and the bridge. Since the triggering mechanism is much faster, a much closer position of the sentinel node to the bridge would have been also feasible. Its location was chosen mostly by practical considerations with the goal to minimize the interference with the business activities in this area.

Due to the lack of line of sight between sentinel node and monitoring nodes, which were mounted below the bridge, two relay nodes were deployed to ensure a safe communication between sentinel node and monitoring nodes. The first relay node was mounted 50 m from the sentinel node on the facade of a building. The second was mounted on the railing of the bridge and provided a safe link to the monitoring nodes below the bridge.

The magnetic sensors of the sentinel node were not placed within the lane such as ILDs but on the roadside (Figure 11). The signal strength is usually smaller but still

Figure 9: The monitored road bridge.

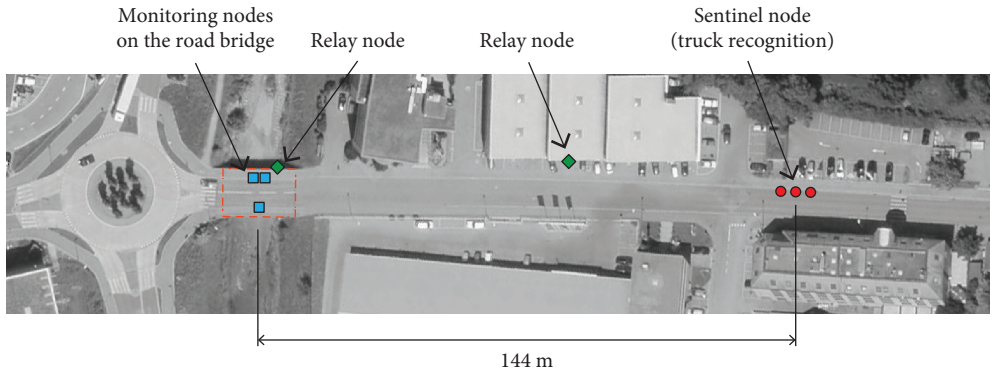

Figure 10: Overview of the test deployment.

(a) (b)

Figure 11: Magnetic field sensors deployed on the roadside.

strong enough to be detectable as demonstrated by the signals displayed in Figure 2. The distance between the magnetic sensors was 4 m. The sonar was mounted on a pole of the road lighting at a height of 2.3 m over the road pavement surface (Figure 12). It was connected with a cable to a single channel sensor node which served as electronic platform for signal conditioning rather than as wireless sensor node. This sensor node was connected with a cable to the multichannel sensor node that received via cable the signals of the magnetic sensors and hosted the truck recognition algorithm. The arrival time of the signals of sonar and magnetic sensors were therefore measured using the same clock.

In order to minimize the intervention on the bridge, only three 120 Ω strain gauges were mounted on the lower concrete surface of the bridge deck. Two were placed in the middle of the span near the edge of the bridge deck that was closest to the lane being monitored by the truck recognition system (Figure 13). One strain gauge was mounted on the opposite edge of the bridge deck. The gauges were protected from humidity.

4.2. WSN Platform. The wireless sensor network is based on the commercial sensor node of the company Decentlab GmbH [20]. The core of the sensor node is the commercial ultra-low-power microcontroller TI MSP430 of Texas Instrument with 256 kB of flash memory, 8 kB of RAM memory, and 16 MHz CPU speed. Wireless delivery of data is enabled using a low-power radio transceiver working in European

Figure 12: Sensor node with sonar mounted on a light pole.

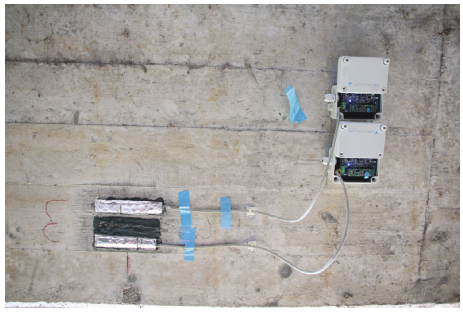

Figure 13: Strain gauges mounted on the concrete surface of the bridge deck and connected to two sensor nodes.

SRD Band from 863 to 870 MHz. The nominal transmission rate is 20 kbit/s. The sleep mode current consumption is 0.6 μW, while during reception and transmission the consumption reaches 27.6 mW and 51 mW, respectively. The platform features a voltage stabilizer that provides a constant input voltage. Fading batteries or voltage fluctuations due to temperature changes do not have any effect on the strain data quality. The WSN nodes were operated using TinyOS2.x.

4.3. Alarming Process. The notification of monitoring about the upcoming event was performed with the flooding protocol that was presented in Popovic et al. [12]. The sentinel node broadcasts an alarm message each time an event, in this case a truck, is detected. The network nodes receiving the alarm message rebroadcasted it up to 3 times in order to ensure that all monitoring nodes received the alarm message. The field test on a railway bridge demonstrated that the notification is fast and reliable: 99.9% of the alarm messages were received by the monitoring nodes after less than 0.5 seconds after being created, and all nodes received the alarm message in time in 98.7% of the events [12].

4.4. Operation Mode. The sentinel node sampled the signal of the three magnetic field sensors with a sampling rate of 123 Hz. The sonar was operated with a pulse rate of 7.5 Hz. The vehicle speed at the position of the sentinel node ranged between 20 and 60 km/h. The length resolution of the sonar was therefore between 0.75 m and 2.22 m and assured a safe detection of high vehicles. For evaluating the hit rate of the truck recognition, a photo camera was installed close to the sentinel node. The remote control terminal of the camera was linked to the sentinel node with a cable. Each time the sonar detected a high vehicle, the sentinel node triggered a picture.

The parameters of length detection were

(i) 5 units for the signal threshold

(ii) 5 samples for the window size

(iii) 20 windows for the counter limit

(iv) 1 s for the detection timer

(v) 6.5 m for the long vehicle threshold

The signal threshold of 5 units was too high for the expected speed. However, at this location the signal noise of the magnetic sensors was about 2 units of RMS. The window size implies a time resolution of 40.7 ms. The theoretical speed estimation error ranges from 1.5 km/h at a vehicle speed of 30 km/h to 3.5 km/h at a vehicle speed of 50 km/h. The average length estimation error induced by the window size is 0.20 m at a vehicle speed of 30 km/h to 0.35 m at a vehicle speed of 50 km/h. The counter limit corresponds to 0.8 s. Such a high value was chosen to improve the identification of long vehicle with low speeds. One second for the detection timer is too great for vehicle speeds between 30 and 50 km/h. Such a value was set to prevent a timeout in order to investigate how frequent a magnetic sensor fails to detect a vehicle. The timers for high and long vehicle detection, which were used for identifying trucks, were set to 1.5 s.

The sentinel node communicated wirelessly the following data to the base station:

(1) The time when a high vehicle was detected

(2) The detection time, the estimated speed and length, and the three signal widths of the magnetic field sensors for each vehicle

(3) The time a truck was detected (height and length thresholds exceeded)

The monitoring nodes were operated in an event-driven mode. Since all recorded raw data was communicated over the network, a small sampling rate of 16 Hz was used to record strains in order to reduce the data size. The data recording of the twin strain gauges on the upper side of the bridge (Figure 10) was operated in two different event-driven modes. While one strain gauge was triggered by the sentinel node and the recording period was 12 s, the other was operated permanently and data records of 4 seconds were triggered only when the strain exceeded a threshold of 5 $\mu\varepsilon$. This software triggering mechanism was described in detail in [6]. On the monitoring nodes, after receiving the alarm the recording was delayed by 5 seconds to compensate for the travel time of the vehicle from the sentinel node to the bridge. The monitoring and relay nodes were operated with a low-power-listening cycle period of 100 ms.

5. Results

5.1. Data Analysis Method. The evaluation of the performance of the sentinel node was performed solely with the data of height and length detection. The main focus of the analysis was on estimating the correct identification of trucks. The recorded data was first sorted according to their time stamps. The time stamp of the height detection was then used as reference since its hit rate for high vehicles was 100%. This was verified by visual observation during the tests and with the pictures of the digital camera that were triggered by the height detection. The detection time of each identified vehicle and the detection time of each identified truck were finally compared to the detection times of a high vehicle. Clearly, the time stamps of height detection did not coincide perfectly with the time stamps of length detection since, first, the length detection algorithm had to wait for the response of the magnetic sensors and, second, the time stamp was provided at the arrival of the data at the base station. Nevertheless, the time gaps were small enough to allow a correct association between the detection of long vehicles and the detection of high vehicles. An additional check was performed by analyzing the previous and following vehicles of correctly detected long vehicles to identify possible false-positive detections.

5.2. Vehicle Classification. During the test period, 231 vehicles were detected. Of these vehicles, 33 (14.3%) were trucks and 6 (2.6%) were delivery vans (Figure 14). The height detection identified correctly all trucks and delivery vans. Contrarily, the length detection identified correctly 26 trucks. Seven trucks were erroneously identified as small cars. This corresponds to a hit rate of 79%. In 3 cases, the vehicle speed was very small (4, 6, and 8 km/h). At such small speeds, the signal gradient within a record is very small so that the vehicle length is significantly underestimated. In the remaining 4 cases, the data analysis did not provide a well-identified cause for the wrong length estimation.

12 short vehicles were erroneously identified as long vehicles by the length detection. These false-positive detections reduced the hit rate of length detection to nearly 60% (Figure 14). In all these cases, the data did not show any anomalies or particularly slow vehicle speeds. One cause of false-positive detection is surely the accuracy of length estimation. Inaccuracy is induced by the window size and the detection threshold. A rough estimation of this inaccuracy can be achieved by analyzing the length estimation variance of the individual sensors for each detected vehicle. This analysis provides an average standard deviation of approximately 0.5 m. This figure is in agreement with the average length estimation error induced by the window size that ranges between 0.2 and 0.35 m.

A standard deviation of 0.5 m, however, is not consistent with 12 incorrectly classified vehicles. Traffic counting stations used vehicle length as a classification criterion. Vehicles with a length up to 5.19 m are classified as passenger cars or motorcycles. By simulating length estimation of vehicles with a length estimation inaccuracy of 0.5 m with a data set of a counting station yields at maximum 1 short vehicle classified as long vehicle. Thus, length estimation inaccuracy is very unlikely to produce the observed classification error.

Another cause of wrong classification can be induced by two closely spaced cars. Such a configuration could be recorded as a long vehicle. Vehicle separation is regulated by the counter limit which was 0.8 s in order to improve the identification of long vehicles with low speeds. Comparing the time gaps between vehicles in the test with time gaps recorded on a traffic counting station reveals that time gaps smaller than 1 s are completely missed in the test data. The smallest recorded time gap is 1.14 s. This result contrasts with the data of the traffic counting station which shows a significant occurrence of time gaps up to 1 s with a local maximum at 0.8 s (Figure 15). The missing time gaps support the hypothesis that the wrong classification was induced by merging two closely spaced cars into a long vehicle. By using a distribution of time gap according to the traffic counting station record and assuming that closely spaced vehicles with a time gap smaller than 1.1 s would be merged into a long vehicle, we obtain 10 wrong vehicle classifications. This result agrees quite well with the observed number of wrong classifications (12).

Finally, 3 delivery vans were classified correctly as short vehicles and 3 were classified as long vehicles. This result is in agreement with a length estimation inaccuracy of about 0.5 m. With an average length of these vehicles of about 6 m, the likelihood of being incorrectly classified is very high.

Additional tests with different configuration parameters did not provide significantly better or poorer hit rates. In tests performed on another road with a speed limit of 80 km/h, length detection performed much better. Of 104 trucks, 100 were correctly identified. This result corresponds to a hit rate of 96%. The discrimination between trucks and delivery vans was also difficult, and the hit rate did not exceed 70%. Since the counter limit was 0.4 s, the identification of two consecutive cars as long vehicle occurred less often (6 cases). In summary, the only satisfactory performance of length detection is primary due to the low speed (the average vehicle speed was

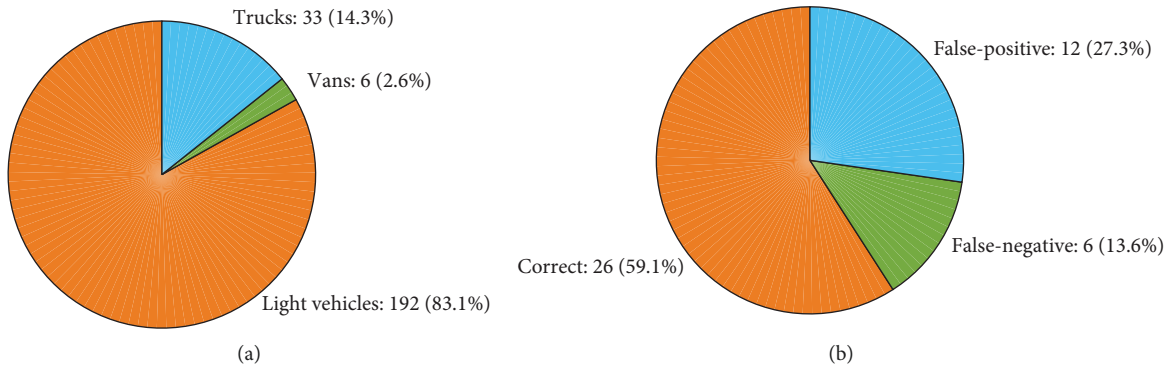

Figure 14: Vehicle classification and performance of length detection.

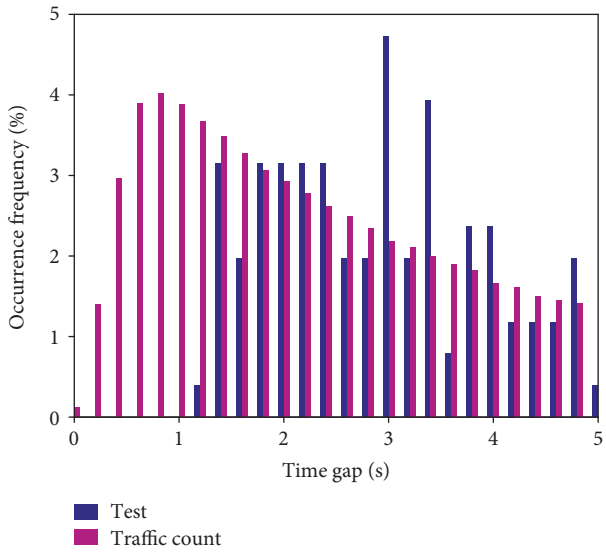

Figure 15: Occurrence frequency of time gap between vehicles.

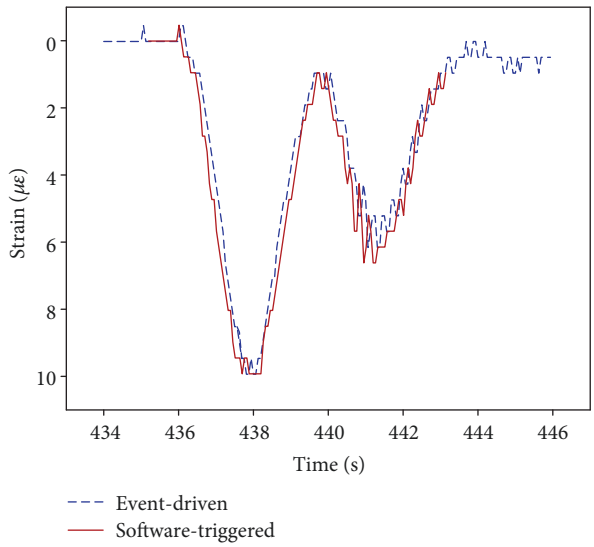

Figure 16: Typical strain records.

about 40 km/h) and the relatively high signal gradient threshold because of the noise.

5.3. Strain Records. A typical strain record is displayed in Figure 16. Even though the sampling rate was rather low, the loading and unloading process is captured very well and with a sufficient resolution. Since the bridge has a natural frequency of about 4 Hz, the sampling rate was able to capture vibrations. The amplitude of the noise spikes is about 0.5 $\mu\varepsilon$.

At the event visualized in Figure 16, the records of the event and software-triggered sensor nodes comply in terms of period and contiguous data. Often this is not the case, since the software-triggered event detection policy kept only records that exceeded the strain threshold of 5 $\mu\varepsilon$. Because of the small-amplitude strain cycles, this policy generated noncontiguous records as visualized in Figure 17 (two records of 4 s width are missing). Noncontiguous records may complicate the computation of the strain cycle amplitudes induced by vehicles since the strain magnitude of the unloaded bridge changes with the temperature. This change was about 6 $\mu\varepsilon$ during the test period. The event-driven recording policy with contiguous records enables to estimate the strain magnitude of the unloaded state. This drawback of the software-triggered event detection policy can be improved by selecting longer record widths (e.g., 8 s instead of 4 s).

6. Conclusions

Event-driven monitoring with sentinel nodes on road bridges is much more demanding than on railway bridges. While for railway bridges the sentinel nodes have just to identify each train independent of its size, for road bridges sentinel nodes have to identify a vehicle and additionally to discriminate between vehicle classes. Furthermore, on roads, the time gap between two vehicles can be very small while trains travelling on the same railway line are separated by minutes. Finally, train speeds at a certain location only exceptionally differ significantly from a standard speed while vehicle speeds on a specific road location may be subjected to great variations.

The proposed sentinel node classifies vehicles by their height and length since their weight, which would be most suitable classification criterion, is too costly to measure. The height detection with sonar is very simple and effective to

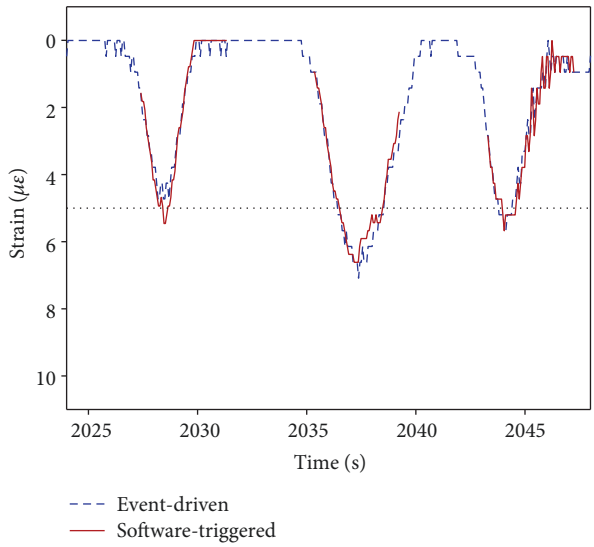

Figure 17: Strain record with data holes.

discriminate between passenger cars or motorcycles and trucks or delivery vans. Since cars are by far the majority of vehicles, usually more than 80%, height detection enables to discard most of the light vehicles.

Length measurement enables also to discriminate between short vehicles (passenger cars and motorcycles) and long vehicles (trucks and delivery vans). In order to improve the effectiveness of event-driven monitoring, length measurement should also be able to discriminate between trucks and delivery vans. The proposed length measurement is rapidly deployable and low-cost but relies on a relatively complex algorithm. This complexity, which is due to the requirement of measuring the length on a moving vehicle, affects the accuracy. The tests show that the achieved accuracy is about 0.5 m. Such an accuracy is sufficient to discriminate trucks from cars but inadequate to distinguish delivery vans from trucks. This discrimination cannot be as effective as distinguishing cars from trucks since the transition from long delivery vans to short trucks is fluent. Swiss vehicle counting stations classify as delivery vans vehicles with a length between 5.2 m and 7.49 m. Vehicles longer than 7.5 m are classified as trucks.

The performance of length measurement depends on vehicle speed. The test suggests that the higher the speed, the better the hit rate. This result is consistent with the theoretical analysis of the length measurement algorithm and is due to the decrease in the signal gradient with decreasing speed. At vehicle speeds smaller than 20 km/h length, detection seems to be quite unreliable. The accuracy of length estimation could be surely improved by calibrating the system parameter in the deployment location. Such a calibration procedure with test vehicles, however, requires additional efforts, time, and costs which may not be compatible with a rapid and low-cost deployment policy.

Considering that delivery vans represent 8 to 10% of vehicles, the question is if the increase in system complexity and deployment costs of the sentinel node due to length estimation is justified. Length estimation requires a deployment of sensors along the road as close as possible to the passing vehicles. For roads with one lane per driving direction, a deployment within the pavement can be avoided. For multilane roads, a deployment within the pavement could be much more difficult to avoid thus requiring greater installation efforts and producing higher costs. On the other side, deployment within the pavement has the benefit of reducing the risk of damages.

A sentinel node with only height detection sonar would be much easier to deploy since it can be placed several meters from the road. By deploying a sentinel node for each lane, height detection works also on roads with several lanes per driving direction. Trucks on the rightmost lane, however, could prevent the sonar to detect a truck travelling in the second lane by reflecting the sonar pulse. Such errors can be avoided by mounting the sonar in the median strip. In such a case, the reporting of height detections wirelessly is the preferred method but, because of the traffic flow, speed and reliability could suffer. Furthermore, a certain filtering of delivery vans could be achieved by mounting the sonar on a higher position than in the tests. In Europe, trucks can reach up to 4 m height. Since smaller delivery vans usually do not exceed 3 m in height, by placing the sonar at a height of 3.5 m many of them could be sorted out. The effectiveness of such an approach needs to be verified by tests, but it should be similar to that of an uncalibrated length estimation. In principle, by increasing the pulse frequency and counting the reflections, even the length could be estimated. Sonar technology, however, has limitations because of the relatively small speed of sound.

In terms of energy consumption, event-driven monitoring with sentinel nodes is always more efficient than a software-triggered policy. The test described in Section 4 had a truck density of 0.64 vehicles per minutes and the recording time was 13% of the elapsed testing time. Even with a significantly higher truck density, event-driven monitoring would have a better energy consumption performance. For roads with an average daily truck density of 2 vehicles per minutes, which is a rather high value, the recording time would be smaller than 50% of the elapsed time. Energy saving of recording would be about a factor 2 which still represents an appreciable goal. On long bridges, the recording time does not necessarily increase, since each monitoring node can be configured with an individual delay time between alarming and recording start. On road bridges, this delay is more difficult to predict since the speed of a vehicle is subjected to greater variations than a train. This uncertainty can be reduced by placing the sentinel node as close as possible to the bridge. In our test, the sentinel node location was selected far away in order to avoid conflicts with the business activity of the area. Critical was the deployment of length estimation sensors since they needed more space and were more exposed to hazards as the height detection sonar.

In summary, event-driven monitoring with sentinel nodes provides advantages over software-triggered event monitoring solution in terms of power saving and finally operation period. On road bridges, however, the disadvantages weigh heavily than those on railway bridges. The accuracy of length estimation needs a significant improvement.

But even with such an improvement, the limitations concerning low vehicle speed and easy and flexible deployability cannot be completely removed. A sentinel node that uses only height detection may finally be a pragmatic solution providing an affordable and reasonable effective filtering of lightweight vehicles.

Data Availability

The data is available on request via the corresponding author.

Conflicts of Interest

The authors declare that they have no conflicts of interest.

Acknowledgments

This investigation was part of the research projects PSRP-124/2010 entitled Innovative Structural Health Monitoring in Civil Engineering Infrastructure Sustainability, Tulcoempa, funded by the Polish-Swiss Research Programme 2009-2017, and the project Hydronet 2, funded by Swiss Electric Research and the Swiss Competence Center Energy and Mobility. The authors express their gratitude to the funding agencies and to the Community of Dietikon for their support during the field tests.

References

[1] M. Liu, D. M. Frangopol, and S. Kim, "Bridge system performance assessment from structural health monitoring: a case study," *Journal of Structural Engineering*, vol. 135, no. 6, pp. 733–742, 2009.

[2] E. Bruehwiler, "Extending the fatigue life of riveted bridges using data from long term monitoring," *Advanced Steel Construction*, vol. 11, no. 3, pp. 283–293, 2015.

[3] J. Leander, A. Andersson, and R. Karoumi, "Monitoring and enhanced fatigue evaluation of a steel railway bridge," *Engineering Structures*, vol. 32, no. 3, pp. 854–863, 2010.

[4] G. Feltrin, K. E. Jalsan, and K. Flouri, "Vibration monitoring of a footbridge with a wireless sensor network," *Journal of Vibration and Control*, vol. 19, no. 15, pp. 2285–2300, 2013.

[5] G. Feltrin, J. Meyer, R. Bischoff, and M. Motavalli, "Long-term monitoring of cable stays with a wireless sensor network," *Structure and Infrastructure Engineering*, vol. 6, no. 5, pp. 535–548, 2009.

[6] G. Feltrin, N. Popovic, K. Flouri, and P. Pietrzak, "A wireless sensor network with enhanced power efficiency and embedded strain cycle identification for fatigue monitoring of railway bridges," *Journal of Sensors*, vol. 2016, Article ID 4359415, 14 pages, 2016.

[7] F. Sutton, R. D. Forno, D. Gschwend et al., "The design of a responsive and energy-efficient event-triggered wireless sensing system," in *International Conference on Embedded Wireless Systems and Networks (EWSN)*, pp. 144–155, Uppsala, Sweden, 2017.

[8] B. Rumberg, D. W. Graham, V. Kulathumani, and R. Fernandez, "Hibernets: energy-efficient sensor networks using analog signal processing," *IEEE Journal on Emerging and Selected Topics in Circuits and Systems*, vol. 1, no. 3, pp. 321–334, 2011.

[9] P. Dutta, M. Grimmer, A. Arora, S. Bibyk, and D. Culler, "Design of a wireless sensor network platform for detecting rare, random, and ephemeral events," in *Proceedings of the 4th International Symposium on Information Processing in Sensor Networks*, pp. 497–502, Los Angeles, CA, USA, 2005.

[10] S. Jevtic, M. Kotowsky, R. P. Dick, P. A. Dinda, and C. Dowding, "Lucid dreaming: reliable analog event detection for energy-constrained applications," in *2007 6th International Symposium on Information Processing in Sensor Networks*, pp. 350–359, Cambridge, MA, USA, 2007.

[11] R. Bischoff, J. Meyer, O. Enochsson, G. Feltrin, and L. Elfgren, "Event-based strain monitoring on a railway bridge with a wireless sensor network," in *4th International Conference on structural health monitoring on Intelligent Infrastructure*, p. 7482, Zurich, Switzerland, 2009.

[12] N. Popovic, G. Feltrin, K.-E. Jalsan, and M. Wojtera, "Event--driven strain cycle monitoring of railway bridges using a wireless sensor network with sentinel nodes," *Structural Control & Health Monitoring*, vol. 24, no. 7, 2017.

[13] Max Botix Inc, *HRXL-Max Sonar®- WR™ Series*, Max Botix Inc, 2012.

[14] J. Gajda, R. Sroka, M. Stencel, A. Wajda, and T. Zeglen, "A vehicle classification based on inductive loop detectors," in *Instrumentation and Measurement Technology Conference, 2001. IMTC 2001. Proceedings of the 18th IEEE*, pp. 460–464, Budapest, Hungary, 2001.

[15] S. Cheung, S. Coleri, B. Dundar, S. Ganesh, C.-W. Tan, and P. Varaiya, "Traffic measurement and vehicle classification with a single magnetic sensor," in *Transportation Research Board. 84th Annual Meeting. 2005, Transportation Research Board*, pp. 1–24, Washington, DC, USA, 2005.

[16] S. Taghvaeeyan and R. Rajamani, "Portable roadside sensors for vehicle counting, classification, and speed measurement," *IEEE Transactions on Intelligent Transportation Systems*, vol. 15, no. 1, pp. 73–83, 2014.

[17] V. Velisavljevic, E. Cano, V. Dyo, and B. Allen, "Wireless magnetic sensor network for road traffic monitoring and vehicle classification," *Transport and Telecommunication Journal*, vol. 17, no. 4, pp. 274–288, 2016.

[18] B. Yang and Y. Lei, "Vehicle detection and classification for low-speed congested traffic with anisotropic magnetoresistive sensor," *IEEE Sensors Journal*, vol. 15, no. 2, pp. 1132–1138, 2015.

[19] Honeywell, *Magnetic Displacement Sensors HMC1501/1512*, Honeywell, 2010.

[20] Decentlab GmbH, *Single Channel Sensor Node*, Decentlab GmbH, 2014.